Comparison of MOF-5 and MIL-101 derived carbons for hydrogen storage application

Tshiamo Segakwenga, Nicholas M. Musyoka[a], Jianwei Ren[*,a], Philip Crouse[*,b], Henrietta W. Langmi[a]

[a]HySA Infrastructure Centre of Competence, Materials Science and Manufacturing, Council for Scientific and Industrial Research(CSIR), P.O Box 395, Pretoria 0001, South Africa.

[b]Department of Chemical Engineering, University of Pretoria, Private Bag x20, Hatfield, 0028, South Africa.

*Corresponding author. Tel: +27 128413450, Email: jren@csir.co.za (J. Ren); Tel: +27 124202856, Email: Philip.Crouse@up.ac.za (P. Crouse)

Abstract

Nanoporous carbons which possess high surface areas and narrow pore size distributions have become one of the most important classes of porous materials with potential to be utilized for hydrogen storage. In recent times, several Metal-organic frameworks (MOFs) have been shown to be promising precursors for creating nanoporous carbons due to their high surface areas and tunable pore sizes. The pore structure and surface area of the resultant carbon materials can be tuned simply by changing the calcination temperature. In this work, a zinc based MOF (MOF-5) and chromium based MOF (MIL-101) were both used as precursors for syntheses of nanoporous carbons structures by direct carbonization technique at different temperatures. The resultant carbon structures possessed high surface areas and differing hydrogen storage capacities.

Keywords: Metal-organic frameworks (MOFs), MOF-5, Cr-MOF (MIL-101), Cr-MOF MDC, MOF-5 MDC, Hydrogen storage

1. Introduction

Hydrogen has for a long time now been regarded as a good energy carrier with the potential to replace the current use of fossil fuels [1]. The current problem restricting the widespread use of hydrogen as a fuel is the lack of an efficient and safe storage system [2]. Ongoing research efforts focused on solid state storage have shown a potential to store hydrogen under cryogenic conditions and the challenge has been to store hydrogen under ambient conditions and at reasonable pressures [3, 4]. Metal-organic frameworks (MOFs) in particular have gained large interest as potential hydrogen storage materials because of their large surface area, pore size that can be tailored to better suit hydrogen storage [5]. MOFS can be integrated into other hydrogen storage applications such as high pressure tanks [6], generation of nanoporous carbons material via carbonization [7] and in electrospinning [8, 9]. Nanoporous carbon materials themselves have also gained much attention as potential hydrogen storage media for the same reasons as MOFs [7, 10, 11]. Porous carbonaceous materials can be synthesized in a variety of ways including direct carbonization of MOFs [7], pyrolysis followed by physical or chemical activation of organic precursors [12], carbonization of polymeric aerogels [11, 13], chemical vapor deposition (CVD) [13], template synthetic procedures [14].

The carbonization of MOFs was first introduced using Zn-based MOFs (MOF-5) to derive porous carbonaceous materials [15]. This carbon synthesis method has been reported by several groups [7, 16]. Currently, most of the work done on the direct carbonization of MOFs has been focused on the Zn-MOFs because removal of the Zn metal species is achieved during the carbonization process. The one challenge to achieving carbonization of MOFs with other metal centres is the removal of the metal after carbonisation.

In this communication, the comparative synthesis of nanoporous carbon materials from MOF-5 and MIL-101 via direct carbonization was explored. The MOF-5 was carbonized at 1000 ^{o}C to vaporize any zinc oxide that may form during the thermal treatment whereas MIL-101 was carbonized at different temperatures (600, 700 and 800 ^{o}C) to find the optimum temperature to carbonize the MOF as well as to remove any oxide material that may form in the pores of the carbon material.

2. Experimental

2.1. Chemicals and reagents

Reagents and chemicals used during the synthesis of both MOF-5 and Cr-MOF were: Zinc nitrate hexahydrate (Sigma-Aldrich, 98%), terephthalic acid (Sigma-Aldrich, 98%), N, N-dimethylformamide (DMF, Sigma Aldrich, 99.8%), anhydrous acetone (Sigma-Aldrich, 99.8%), N_2 gas (Air Products, South Africa, 99.9995%), Chromium chloride hexahydrate ($CrCl3{\cdot}6H_2O$, Sigma Aldrich, 99.5 %), formic acid (HCOOH, Sigma Aldrich, 95 %). De-ionized water was obtained from a water purification system (Instrubal, Zeneer Power II) in the laboratory. These reagents were purchased and used without further purification.

2.2. Synthesis of MOF-5

The procedure for the synthesis of MOF-5 is the same as reported previously [17]. Typically, experiments were conducted using a 250 ml round-bottom flask and an oil bath to provide constant reaction temperature. The synthesis apparatus was composed of a round-bottomed flask equipped with a reflux condenser and an elliptical teflon-lined stirrer (10×19 mm). In the flask, 0.665 g (4 mmol) of terephthalic acid and 3.13 g (10.52 mmol) zinc nitrate hexahydrate were dissolved in 100 ml of DMF solvent. The flask was under a continuous flow of N_2 gas while being heated up to 140 ^{o}C and this temperature was maintained for 4 h with stirring at 1000 rpm. After the reaction was complete, the flask was cooled down to room temperature, and then the product was filtered off. The resulting product was ultrasonically washed with acetone and dried at 120 ^{o}C for 24 h under vacuum then further dried at 200 ^{o}C for 24 h under vacuum.

2.3. Synthesis of MIL-101

The synthesis procedure for producing MIL-101 was previously reported [18]. Typical experiments were conducted using a 250 ml Teflon-lined Berghof high-pressure reactor (Heizüng, Germany). To prevent the formation of MIL-53, the synthesis time was kept to 8 h and a molar ratio of $CrCl_3.6H_2O/H_2BDC/550H_2O$ for the reaction constituents was maintained. For this reaction, 0.83 g (5 mmol) of terephthalic acid and 1.33 g (5 mmol) of chromium chloride were dissolved in 50 ml (2.78 mol) of de-ionized water with the help of

an ultrasonic bath. Thereafter, 33 ml (2.78 mol) of formic acid was added as the modulator. The reaction mixture was then transferred to the high-pressure reactor and heated to 210 °C and held at that temperature for 8 h. When the reaction was complete, the reactor was cooled to room temperature and the products were collected by centrifugation. The synthesis products were a mixture of green powder and colourless needle-like recrystallized terephthalic acid. The acid was removed by washing the products in hot DMF at 80 °C for 1 h. The remaining green powder was then collected and dried under vacuum at room temperature.

2.4. Synthesis of MOF-5 and Cr-MOF derived carbons

The MOF-derived carbons from the two kinds of MOFs were prepared by direct carbonization procedure. For MOF-5, only one carbonization temperature was investigated (1000 °C) whereas Cr-MOF was investigated at 600, 700 and 800 °C. The as-synthesized MOFs were independently put in an alumina boat and placed in a tube furnace. The furnace was heated from room temperature to the set temperature under Ar flow at the rate of 5 °C/min, and thereafter maintained at that temperature for 5 h. No further preparation steps were conducted for MOF 5-derived carbon samples. But upon noticing that there was still presence of Cr in the Cr-MOF based carbon samples, further post-synthesis acid treatments were conducted using either HF or HCl. The resulting Cr-MOF derived carbonaceous samples were labelled as MDC-600, MDC-700 and MDC -800.

2.5. Characterization

Powder diffraction patterns for all samples were collected at room temperature using a PANalytical X'Pert Pro powder diffractometer with Pixcel detector using Ni-filtered Cu K-alpha radiation (0.154 nm) in the range of 2θ=1–80°, and scanning rate of 0.1 °/s. The exposure time of sample to environment was about 20 min including the sample preparation and testing procedure. Surface area and pore characteristics measurements were carried out on an ASAP 2020 HD analyser (Micromeritics), and the p/p_0 range chosen for BET surface area determination was 0.05–0.2. H_2 adsorption isotherms at 77 K and up

to 1 bar were also measured on ASAP 2020 instrument. All gas sorption isotherms were obtained using ultra-high pure gas (99.999%). Prior to the ASAP analysis, 0.1–0.3 g of each sample was outgassed overnight at 300 ^{o}C for MOF-5, 200 ^{o}C for Cr-MOF and the carbonised samples. Each sample was outgassed under vacuum down to a pressure of 10^{-5} bar. The outgassing was enough to remove all solvent molecules without compromising the integrity of the structures of each sample. A scanning electron microscope (SEM; JEOL-JSM 7500F) was used to study the morphology of the samples.

2. Results and discussion

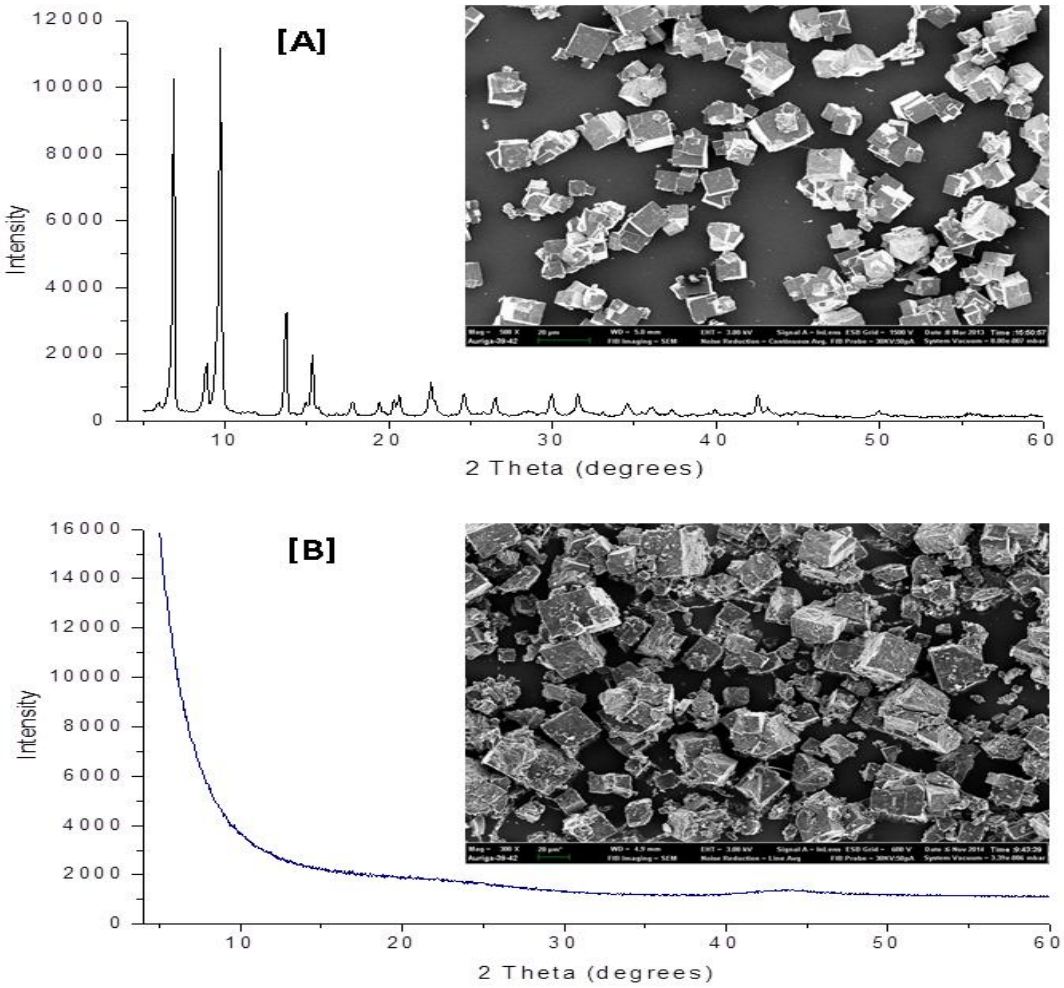

Figure 1: XRD patterns and the respective SEM images of [A] MOF-5 and [B] MOF-5 MDC

The XRD patterns for MOF-5 and MOF-5 MDC are shown in Figure 1a and 1b respectively, with their respective SEM images shown as the inserts. The successful synthesis of MOF-5 was confirmed by XRD spectra as previously reported [17, 18]. The SEM images showed nearly regular cube shaped crystals. After carbonization, all peaks corresponding to the pristine MOF-5 completely disappeared, indicating that the obtained carbon was nearly amorphous [7]. In this case, the MOF precursor for MOF-5 was completely decomposed and the Zn converted to zinc oxide (ZnO) which was then reduced to Zn at 900 $^{\circ}$C allowing the evaporation of the Zn and achieving highly porous carbon.

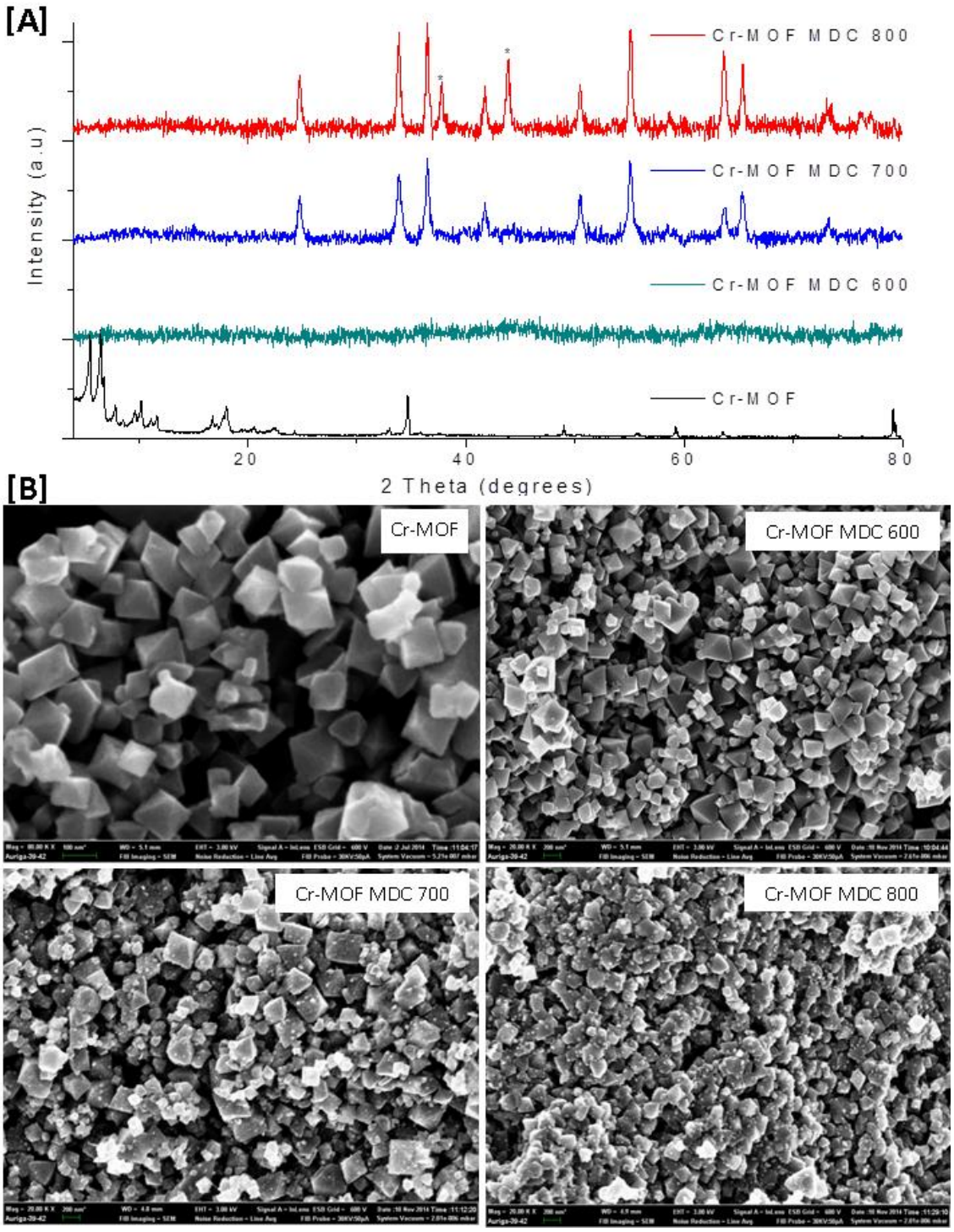

Figure 2: PXRD and SEM images of Cr-MOF MDC

On the other hand, the XRD pattern and SEM images of Cr-MOF shown in Figure 2 corresponded well with those earlier reported in the literature [18]. The Cr-MOF derived carbons samples produced at different temperatures MDC-600, MDC-700 and MDC-800 (Figure 2b) were observed to have retained the octahedral cubic morphology of the

pristine Cr-MOF with the sharpness of the edges decreasing as the temperature was increased. From the XRD patterns, Cr-MOF MDC carbonized at 800 ^{o}C had peaks at 2θ = 38 and 44^{o} that corresponded to the presence of Cr carbide whereas the other peaks were for Cr oxide. The XRD spectrum for the MDC-700 sample did not show peaks related to the carbide and only the chromium oxide could be identified. Upon reduction of the carbonization temperature to 600 ^{o}C (MDC-600), neither chromium carbide or oxide was observed. This indicated that the MDC-600 was amorphous although the morphology was maintained and the internal structure had completely collapsed. Attempts to remove the chromium carbide and oxide from Cr-MOF derived carbons was conducted using both HCl and HF acids by refluxing the samples for 4 h at 65 °C in 5M HCl. However, it is evident from the TGA curves shown in Figure 3a that the acid washing was not effective enough in removing the metallic species. This observation is also corroborated by the EDS elemental scanning shown in Figure 3b-d.

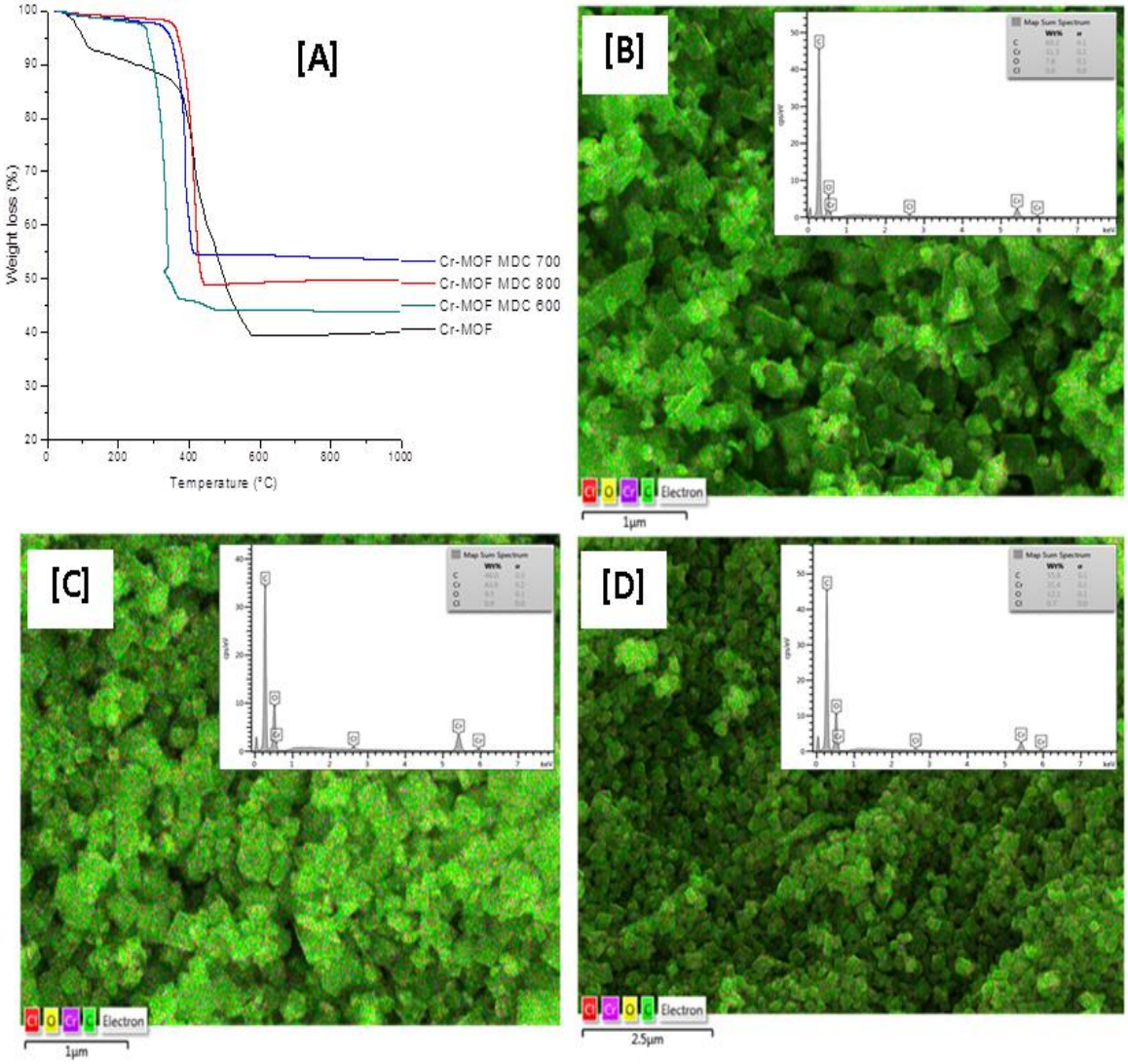

Figure 3: TGA plots [A] and EDS elemental mapping [B-D] of Cr-MOF and its derived carbon at different carbonization temperatures (600 – 800 °C)

The mass loss observed from the derived carbons from the Cr-MOF (Figure 3a) was relatively lower when compared to that of pristine Cr-MOF and this can be explained by the structural changes that were induced by the carbonisation process. Even though Ming et al. [19] had reported that porous carbons obtained from MOFs consisting of metals with higher boiling points than Zn (such as Fe, Co, Cu) could retain the metallic species, and they could be removed from the resulting carbons after being washed with acid [19]. Although as stated, it is evident from this study that Cr oxide and formed carbides were very difficult to be removed and hence Cr-MOF carbonisation is not recommended for this type of MOF.

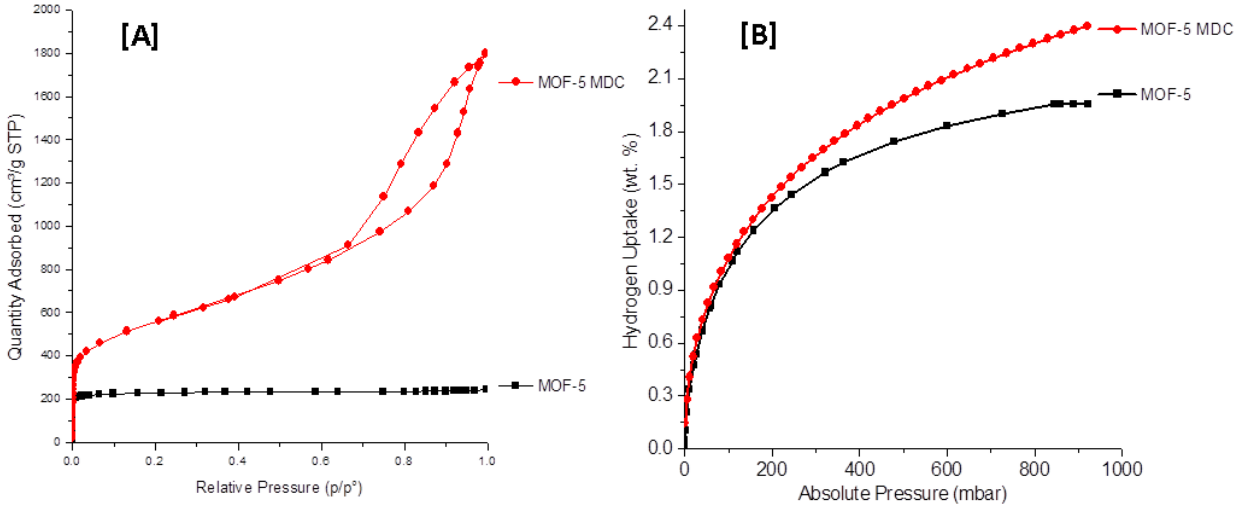

Figure 4: Nitrogen sorption isotherms [A] and hydrogen uptake isotherms [B] for MOF-5 and MOF-5 MDC.

The nitrogen sorption isotherm (at 77 K and I bar) for pristine MOF-5 sample (Figure 4a) was observed to be of Type I in nature which indicative of a microporous sample. The MOF-5 MDC isotherm, on the other hand, was observed to be Type IV in nature. The hysteresis observed at the higher partial pressure of MOF-5 MDC sample indicated that the derived carbon sample had some mesoporosity [20]. From Table 1, the measured surface area for the MOF-5 was 981 $m^2.g^{-1}$ and whereas that of MOF-5 MDC was 2393 $m^2.g^{-1}$. The pore volumes for MOF-5 were found to be 0.3 $cm^3.g^{-1}$ whereas those of the MOF-5 MDC were 1.13 $cm^3.g^{-1}$. At 77 K and up to a pressure of 1 bar, the H_2 adsorption for the synthesized MOF-5 and its MDCs were found to be 1.9 wt.% and 2.7 wt.%, respectively. The enhancement can be explained by differences in the textural and structural characteristics of the two samples. In this case, the pristine MOF-5 was microporous and after carbonization, the MDC sample was found to possess a higher degree of microporosity and also enhanced surface area. Studies by Yang et al. [7] had proved that MOF carbonisation leads to development of ultramicroporosity which is thought to be the reason for the enhanced H_2 storage capacity in this case.

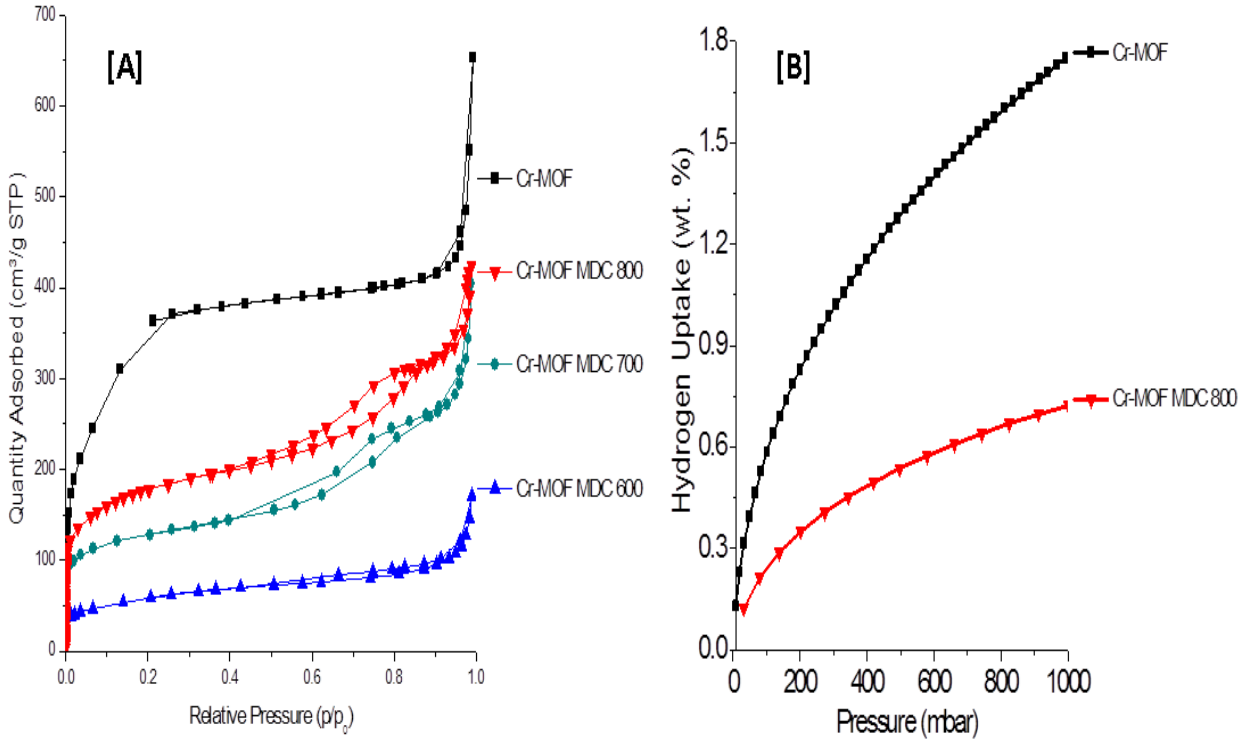

Figure 5: Nitrogen sorption isotherms [A] and Hydrogen uptake isotherms [B] for Cr-MOF and Cr-MOF MDC samples obtained at 600, 700 and 800 °C.

Contrary to the observation for MOF-5 MDC, the nitrogen sorption isotherms (at 77 K and 1 bar) for the pristine desolvated Cr-MOF sample was observed to be of Type IV in nature which indicated that the sample had both micro and meso porous. The MDC samples were also found to be of Type IV but the degree of enlargement of the hysteresis loop was higher as the carbonisation temperature increased. This observation indicated that the samples were becoming more mesoporous with the increased carbonisation temperature. From Table 1, it can be observed that the surface area for the entire Cr-MOF MDC sample obtained at different carbonisation temperatures was lower than the pristine starting Cr-MOF. In this case, Cr-MOF MDC 600 was found to adsorb the lowest amount of N_2 which was indicative of the collapsed pores. It also had the lowest BET surface area of the three MDC sample (202 $m^2.g^{-1}$) and the lowest pore volumes (0.0.27 $cm^3.g^{-1}$). The other two MDC samples of MDC-700 and MDC-800 had BET surface areas of 461 $m^2.g^{-1}$ and 628 $m^2.g^{-1}$, respectively. Based on this information, the hydrogen uptake of the MDC sample with the highest surface area and pore volumes was chosen for further investigated for its

H_2 storage properties.

The H_2 storage isotherms (at 77 K and up to a pressure of 1 bar) for the synthesized Cr-MOF and Cr-MOF MDC-800 sample are presented in Figure 5b. The H_2 adsorption for the Cr-MOF was found to be 1.9 wt.% whereas that of Cr-MOF MDC 800 sample was 0.9 wt.%. The H_2 sorption isotherms for the pristine Cr-MOF sample showed a steep increase at low pressure up to 1 bar and did not reach saturation which was an indication that at higher pressures it would be possible to achieve higher H_2 storage capacities. Unlike in the case with the MOF-5 MDC sample, the hydrogen uptake did not increase and instead a decrease by about 47 % compared to that of Cr-MOF. This decrease can be explained by the presence of the carbide and chromium oxide in the pores of the MDC sample which restricted the space available for the H_2 to occupy hence the lowered hydrogen uptake. A decrease of this magnitude for the MDC-800 sample, which had the highest surface area and pore volumes of the three MDC samples, meant that the other two samples would also have even lower H_2 adsorption which would make them impractical for H_2 storage application. Therefore, the H_2 storage capacity of the MDC-600 and MDC-700 samples was not measured. Unlike with MOF-5, the direct carbonization of Cr-MOF did not result in increased H_2 storage capacities as removing the chromium oxide or the carbide from the pores of the MDC was nearly impossible. Although the reduction in carbonising temperature limited the production of the oxide and carbide, it also resulted in a sample with very low porosity. Table 1 summarizes the textural parameters and hydrogen uptake capacities of all the samples investigated in this study.

Table 1: Cr-MOF and Cr-MOF MDC morphology characteristics

Sample ID	S_{BET} ($m^2.g^{-1}$)	S_{Lang} ($m^2.g^{-1}$)	Pore Vol. ($cm^3.g^{-1}$)	Micro. Vol. ($cm^3.g^{-1}$)	H_2 uptake (wt. %)
Cr-MOF	2619	3485	1.36	1.22	1.9
MDC-600	202	237	0.027	0.025	-
MDC-700	461	524	0.036	0.038	-

MDC-800	628	826	0.54	0.11	0.8
MOF-5	835	992	0.38	0.24	1.9
MOF-5 MDC	2393	2738	1.13	0.34	2.7

3. Conclusions

In conclusion, two kinds of MOFs were used as templates for carbon nanostructures. The carbonised MOF-5 sample had increased surface area from 835 $m^2.g^{-1}$ to 2393 $m^2.g^{-1}$ and also enhanced H_2 storage capacity from 1.9 to 2.7 wt.%. On the contrary, the carbonised Cr-MOF samples showed a decrease in both the surface area and hydrogen uptake capacities when compared to that of pristine Cr-MOF. This decline in the Cr-MOF MDC properties can be attributed to the presence chromium oxide and carbide in the pores. It can thus be concluded that Cr-MOF carbonisation would not be an appropriate route for generating porous carbons with good hydrogen storage capacity since the pores were either occupied by the chromium oxide, the carbide or were collapsed and thus hindering the adsorption of any guest molecules.

Acknowledgements

The financial support from the South African Department of Science and Technology (DST) towards HySA project (Grant No.: HTC004X) is gratefully acknowledged.

References

1. Sandrock G. A panoramic overview of hydrogen storage alloys from a gas reaction point of view. J Alloys Compounds 1999;293:877-88.

2. Schlapbach L. Technology: Hydrogen-fuelled vehicles. Nature 2009;460(7257):809-11.

3. Yaghi OM, O'Keeffe M, Ockwig NW, Chae HK, Eddaoudi M, Kim J. Reticular synthesis and the design of new materials. Nature 2003;423:705-14.

4. Rosi NL, Eckert J, Eddaoudi M, Vodak DT, Kim J, O'Keeffe M, et al. Hydrogen storage in microporous metal-organic frameworks. Science 2003;300:1127-9.

5. Furukawa H, Cordova KE, O'Keeffe M, Yaghi OM. The chemistry and applications of metal-organic frameworks. Science 2013;341:1230444.

6. Takeichi N, Senoh H, Yokota T, Tsuruta H, Hamada K, Takeshita HT, et al. “Hybrid hydrogen storage vessel”, a novel high-pressure hydrogen storage vessel combined with hydrogen storage material. Int J Hydrogen Energy 2003;28:1121-9.

7. Yang SJ, Kim T, Im JH, Kim YS, Lee K, Jung H, et al. MOF-derived hierarchically porous carbon with exceptional porosity and hydrogen storage capacity. Chemistry of Materials 2012;24:464-70.

8. Reardon H, Hanlon JM, Hughes RW, Godula-Jopek A, Mandal TK, Gregory DH. Emerging concepts in solid-state hydrogen storage: the role of nanomaterials design. Energy & Environmental Science 2012;5:5951-79.

9. Rose M, Böhringer B, Jolly M, Fischer R, Kaskel S. MOF processing by electrospinning for functional textiles. Advanced Engineering Materials 2011;13:356-60.

10. Tsuruoka T, Furukawa S, Takashima Y, Yoshida K, Isoda S, Kitagawa S. Nanoporous Nanorods Fabricated by Coordination Modulation and Oriented Attachment Growth. Angewandte Chemie International Edition 2009;48:4739-43.

11. Yang Q, Xu W, Tomita A, Kyotani T. The template synthesis of double coaxial carbon nanotubes with nitrogen-doped and boron-doped multiwalls. J Am Chem Soc 2005;127:8956-7.

12. Journet C, Maser W, Bernier P, Loiseau A, de La Chapelle, M Lamy, Lefrant dlS, et al. Large-scale production of single-walled carbon nanotubes by the electric-arc technique. Nature 1997;388:756-8.

13. Zheng B, Lu C, Gu G, Makarovski A, Finkelstein G, Liu J. Efficient CVD growth of single-walled carbon nanotubes on surfaces using carbon monoxide precursor. Nano Letters 2002;2:895-8.

14. Ahmadpour A, Do D. The preparation of active carbons from coal by chemical and physical activation. Carbon 1996;34:471-9.

15. Yang SJ, Kim T, Im JH, Kim YS, Lee K, Jung H, et al. MOF-derived hierarchically porous carbon with exceptional porosity and hydrogen storage capacity. Chemistry of Materials 2012;24:464-70.

16. Liu B, Shioyama H, Akita T, Xu Q. Metal-organic framework as a template for porous carbon synthesis. J Am Chem Soc 2008;130:5390-1.

17. Ren J, Rogers DE, Segakweng T, Langmi HW, North BC, Mathe M, et al. Thermal treatment induced transition from $Zn_3(OH)_2(BDC)_2$(MOF-69c) to $Zn_4O(BDC)_3$(MOF-5). International Journal of Materials Research 2014;105:89-93.

18. Ren J, Musyoka NM, Langmi HW, Segakweng T, North BC, Mathe M, et al. Modulated synthesis of chromium-based metal-organic framework (MIL-101) with enhanced hydrogen uptake. Int J Hydrogen Energy 2014;39: 12018-23.

19. Hu M, Reboul J, Furukawa S, Torad NL, Ji Q, Srinivasu P, et al. Direct carbonization of Al-based porous coordination polymer for synthesis of nanoporous carbon. J Am Chem Soc. 2012;134:2864-7.

20. Hirscher M, Panella B, Schmitz B. Metal-organic frameworks for hydrogen storage. Microporous and mesoporous materials 2010;129:335-9.

21. Dueren T, Millange F, Ferey G, Walton KS, Snurr RQ. Calculating Geometric Surface Areas as a Characterization Tool for Metal-Organic Frameworks. Journal of Physical Chemistry 2007;111:15350-56.